Proceedings of V&V Verification and Validation Symposium
V&V 2020
May 20-22, 2020, Baltimore, USA

VVS2020-13055

ON THE ROLE OF DISCRETIZATION ERRORS IN THE QUANTIFICATION OF PARAMETER UNCERTAINTIES

Luís Eça
MARIN Academy, IST ULisbon
Email: luis.eca@tecnico.ulisboa.pt

Filipe S. Pereira
Los Alamos National Laboratory
Email:fspereira@lanl.gov

Guilherme Vaz
WavEC Offshore Renewables
Email:guilherme.vaz@wavec.org

Rui Lopes
IST ULisbon
Email:rui.a.lopes@tecnico.ulisboa.pt

Serge Toxopeus
MARIN
Email:S.L.Toxopeus@marin.nl

ABSTRACT

The independence of numerical and parameter uncertainties is investigated for the flow around the KVLCC2 tanker at $Re = 4.6 \times 10^6$ *using the time-averaged RANS equations supplemented by the* $k-\omega$ *two-equation SST model. The uncertain input parameter is the inlet velocity that varies* $\pm 0.25\%$ *and* $\pm 0.50\%$ *for the determination of sensitivity coefficients using finite-difference approximations. The quantities of interest are the friction and pressure coefficients of the ship and the Cartesian velocity components and turbulence kinetic energy at the propeller plane.*

A grid refinement study is performed for the nominal conditions to allow the estimation of the discretization error with power series expansions. However, for grids between 6×10^6 *and* 47.6×10^6 *cells, not all the selected quantities of interest exhibit monotonic convergence. Therefore, the estimates of the sensitivity coefficients of the selected quantities of interest using the local sensitivity method and finite-differences performed for refinement levels that correspond to* 0.764×10^6, 6×10^6 *and* 47.6×10^6 *cells lead to significantly different values. Nonetheless, for a given grid, negligible differences are obtained for the sensitivity coefficients obtained with two different intervals in the finite-differences approximation.*

Discrepancies between sensitivity coefficients are compared with the estimated numerical uncertainties. Results obtained in the study suggest that uncertainty quantification performed in coarse grids may be significantly affected by discretization errors.

INTRODUCTION

In a study presented in the V&V Symposium of 2019 [1], the independence of numerical and parameter uncertainties was investigated for two-dimensional, incompressible flows over a flat plate and around an airfoil. The simulations were performed with the RANS equations supplemented by eddy-viscosity and transition models and the uncertain input condition was the level of eddy-viscosity at the inlet. In that study, sets of geometrically similar grids were used with a level of grid refinement that allowed reliable estimates of the discretization error (iterative and round-off errors are negligible) using power series expansions. The results suggested that independence of parameter and numerical uncertainties requires attaining smooth convergence with grid refinement, i.e. when the data approaches the so-called asymptotic range.

In the simulation of high Reynolds numbers (turbulent) flows around complex geometries, attaining such level of grid refinement (the asymptotic range) is still rare. On the other hand, uncertainty quantification (UQ) is becoming common practice in engineering applications. However, in many cases it is assumed that the propagation of input uncertainties through a flow solver (one of the most common applications of UQ) is independent

of the discretization error. Therefore, in the interest of saving computational time, uncertainty quantification estimates are often performed with grid refinement levels that lead to significant discretization[1] errors.

This paper repeats the exercise reported in [1] with one main difference: the test case is the flow around the KVLCC2 tanker at Re$= 4.6 \times 10^6$, which can be considered a practical test case. In the present exercise, the uncertain input parameter is the inlet velocity that varies $\pm 0.25\%$ and $\pm 0.50\%$. The study is performed with the same options used in [1]: estimates of the sensitivity coefficients of the selected quantities of interest are made using the local sensitivity method and finite-differences [2]; the flow solver is ReFRESCO [3] that is based on a finite volume discretization of the Reynolds-Averaged continuity and Navier Stokes equations (RANS) supplemented by the two-equation $k-\omega$ Shear-Stress Transport (SST) eddy-viscosity turbulence model [4].

The flow around the KVLCC2 tanker at model scale Reynolds number has been studied experimentally [5] in a wind tunnel using the so-called double body approach. This means that a symmetric model was used with the symmetry plane located at the still water plane. The main focus of the experimental work was the measurement of the velocity field at six different cross-stream sections at the stern and wake of the ship. For the present exercise, we have selected as quantities of interest the three Cartesian velocity components V_x, V_y and V_z and the turbulence kinetic energy k at the 654 locations where experimental data is available. Furthermore, we have also considered the friction C_F and pressure C_P resistance coefficients (integral quantities) as quantities of interest.

Flow simulations were performed for a set of 10 nearly geometrical similar multi-block structured grids covering a grid refinement ratio $r = h_i/h_1$ of approximately 4, where h_i is the typical cell size of grid i. Discretization errors of the quantities of interest are estimated with the power law fits presented in [6] using the data of the 6 finest grids that cover a grid refinement ratio of 2. On the other hand, the sensitivity coefficients of the quantities of interest are determined for three grid refinement levels: $r = 1$, $r = 2$ and $r = 4$. Furthermore, the finite-differences approximations are performed with two different intervals of the uncertain input parameter to assess the accuracy of the determination of the sensitivity coefficients for a given grid. These results will allow us to evaluate the influence of the discretization error on the determination the sensitivity coefficients, which is different from evaluating the accuracy of using finite-difference approximations to evaluate sensitivity coefficients for a given grid.

The remainder of this paper is organized in the following way: the test case (governing equations, domain size and boundary conditions) is described in the following section that also contains the definition of the quantities of interest; next, a brief description of the flow solver is presented including the numerical settings used in the present work; the following section presents the grids sets, the estimation of the numerical errors and the results obtained for the sensitivity coefficients with the three grid refinement ratios selected; the last section presents the main conclusions of this study.

[1]It should be mentioned that iterative errors may also pollute the numerical solution, but iterative convergence criteria in UQ studies are rarely mentioned.

TEST CASE

Governing equations

The time-averaged RANS equations for an incompressible fluid are written in strong conservation form as

$$\begin{aligned} &\frac{\partial V_i}{\partial x_i} = 0 \\ &\frac{\partial}{\partial x_j}\left(\rho V_i V_j\right) = -\frac{\partial p}{\partial x_i} + \frac{\partial \tau_{i,j}}{\partial x_j} \end{aligned} , \tag{1}$$

where the coordinates of a Cartesian coordinate system $(x_1, x_2, x_3) \equiv (x, y, z)$, $(V_1, V_2, V_3) \equiv (V_x, V_y, V_z)$ and ρ is the fluid density. The stress-tensor $\tau_{i,j}$ is determined using the eddy-viscosity μ_t hypothesis that leads to the effective viscosity

$$\mu_{ef} = \mu + \mu_t \, , \tag{2}$$

with μ as the fluid dynamic viscosity.

$$\tau_{i,j} = \mu_{ef}\left(\frac{\partial V_i}{\partial x_j} + \frac{\partial V_j}{\partial x_i}\right) . \tag{3}$$

Gravity and part of the normal Reynolds stresses are absorbed in p, which is defined by

$$p = P - P_h + \frac{2}{3}k \, , \tag{4}$$

where P is the average static pressure, P_h is the hydrostatic pressure and k is the turbulence kinetic energy. The eddy-viscosity is determined with the two-equation $k-\omega$ SST model [4] that solves two extra transport equations for k and the turbulence frequency ω to determine

$$\nu_t = \frac{\mu_t}{\rho} = \frac{a_1 k}{\max\left(a_1\omega, F_2 S\right)} . \tag{5}$$

S is the mean strain-rate and the model constants (including a_1) and blending functions of the model (including F_2) are given in [4].

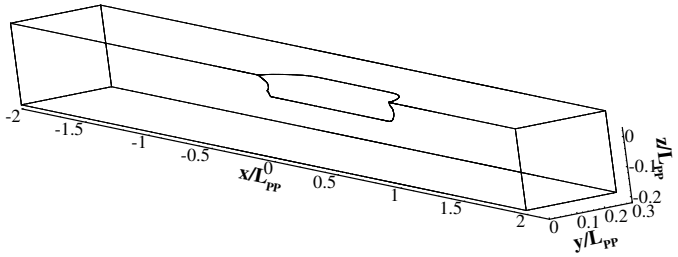

FIGURE 1. Illustration of the computational domain and reference frame used in the calculation of the flow around the KVLCC2 tanker at model scale Reynolds number.

Geometry and computational domain

The KVLCC2 tanker is a classical test case from the Workshops on CFD in Ship Hydrodynamics [7, 8]. At model scale, the Reynolds number based on undisturbed velocity V_∞, distance between perpendiculars L_{PP} and kinematic viscosity ν is $Re = 4.6 \times 10^6$. The flow around the KVLCC2 tanker has been extensively studied using RANS and several turbulence models in [9, 10].

The computational domain is a rectangular prism defined in a Cartesian coordinate system with x aligned with the incoming flow (pointing to the bow), the transverse y axis perpendicular to the symmetry plane of the ship ($y = 0$) and the vertical direction z forming a right-handed system. The origin of the reference frame is located at the intersection of the symmetry plane of the ship, the keel line and the aft perpendicular, as illustrated in Fig. 1.

The cross-section of the computational domain replicates the dimensions of the wind tunnel used by Lee et al. [5]. Due to the two symmetry planes of the tested geometry, only one quarter of the double-body ship is modeled. This leads to a cross-section of $0.33L_{PP}$ width and $0.27L_{PP}$ height with the symmetry planes located at $y = 0$ and $z = 0.065L_{PP}$ (still water plane). The length of the domain is $4L_{PP}$ with the inlet boundary placed at $x = 2L_{PP}$.

Boundary conditions

The computational domain includes seven boundaries where boundary conditions must be specified: inlet plane; outlet plane; surface of the ship; symmetry plane of the ship; lateral boundary; bottom boundary and still water plane. Unfortunately, exact boundary conditions are the exception instead of the rule. Nonetheless, we have considered only one uncertain boundary condition which is V_x at the inlet of the computational domain.

At the inlet boundary, $V_x = V_\infty$, $V_y = 0$, $V_z = 0$ and the pressure is extrapolated from the interior. k and ω are derived from the reported experimental turbulence intensity $I = 0.15\%$ [5] and a ratio between turbulent and molecular kinematic viscosities of

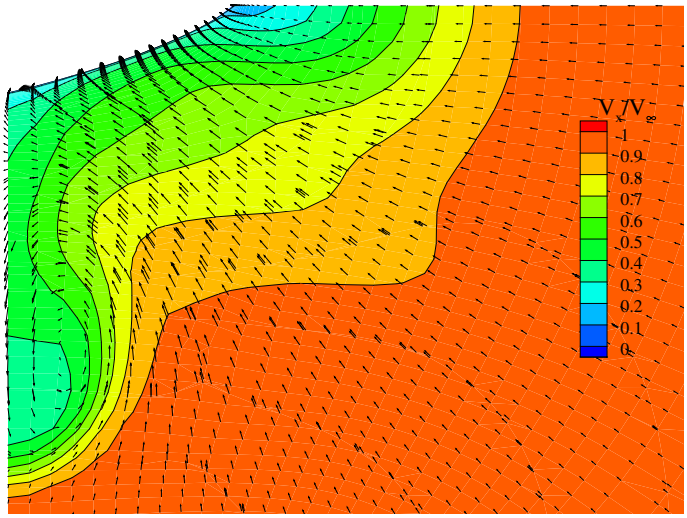

FIGURE 2. Isolines of the axial velocity component V_x and transverse velocity field at the propeller plane $x = 0.0175L_{PP}$ of the flow around the KVLCC2 tanker at model scale Reynolds number.

$\nu_t/\nu = 0.01$. Sensitivity coefficients of the quantities of interest are determined for intervals of $\pm 0.25\%$ and $\pm 0.5\%$ of V_x.

The pressure is imposed at the outflow boundary and the streamwise derivatives of the remainder dependent variables are set equal to zero. At the lateral ($y = 0.33L_{PP}$) and bottom $z = -0.207L_{PP}$ boundaries, the normal velocity component is set equal to zero (V_z for the lateral boundary and V_y for the bottom boundary) and the derivatives with respect to the normal direction (z for the lateral boundary and y for the bottom boundary) of the remainder dependent quantities are set equal to zero.

Velocity components are set equal to zero at the ship surface due to the no-slip and impermeability conditions. The pressure derivative in the direction normal to the ship surface and k are set equal to zero, whereas ω is specified at the nearest wall cell centre [11] using its near-wall analytic solution [12]. The shear-stress at the wall is calculated from its definition, i.e. without wall-functions.

Symmetry conditions are prescribed at the top boundary ($z = 0.065L_{PP}$) and symmetry plane of the ship ($y = 0$) .

Quantities of interest

Two types of flow quantities were selected to check the dependence of the sensitivity coefficients on the discretization error: the friction C_F and pressure C_P resistance coefficients obtained from the integration of the shear-stress at the wall and pressure on the ship surface; the Cartesian velocity components V_x, V_y and V_z and the turbulence kinetic energy k at the 654 locations of the propeller plane $x = 0.0175L_{PP}$, where experimental data is available [5]. The isolines of V_x and the transverse field

at the propeller plane are illustrated in Fig. 2. The flow exhibits a reduction of V_x at the centre of the bilge vortex that is essential for the design of the ship propeller.

FLOW SOLVER

ReFRESCO (`www.refresco.org`) is a community based open-usage CFD code for the Maritime World. It solves multiphase (unsteady) incompressible viscous flows using the Navier-Stokes equations, complemented with turbulence models, cavitation models and volume-fraction transport equations for different phases [13]. The equations are discretized using a finite-volume approach with cell-centered collocated variables, in strong-conservation form, and a pressure-correction equation based on the SIMPLE algorithm is used to ensure mass conservation. The non-linear system of equations[2] for velocity and pressure is linearized with Picards method and either a segregated or coupled approach is used. In the latter, the coupled linear system is solved with a matrix-free Krylov subspace method using a SIMPLE-type preconditioner [14]. A segregated approach is adopted for the solution of all other transport equations. The implementation is face-based, which permits grids with elements consisting of an arbitrary number of faces (hexahedra, tetrahedral, prisms, pyramids, etc.), and if needed h-refinement (hanging nodes). Volume and surface integrals are calculated with second-order mid-point rules and pressure-weighted interpolation [15] is applied for the calculation of the mass fluxes at the faces centre. Several schemes are available for the approximation of the convective and diffusive fluxes (selected schemes are given below). ReFRESCO is currently being developed and verified [16] at MARIN (in the Netherlands), in collaboration with IST (in Portugal) and other non-profit organizations around the world.

Numerical settings

Second-order schemes were selected for the discretization of the convective and diffusive fluxes of all transport equations, except the k and ω convective fluxes that are approximated with first-order upwind schemes. Non-orthogonality corrections are applied to the diffusive fluxes and eccentricity corrections are used in the determination of gradients at the cells centre using Gauss's theorem.

All calculations are performed in double precision and so the contribution of the round-off error to the numerical error is negligible. Furthermore, iterative convergence requires a maximum value (L_∞) of the normalized residuals below 10^{-8}, which corresponds to mean values of the normalized residuals below approximately 10^{-10}. For each transport equation, residuals are normalized by the main diagonal of the matrix of coefficients and divided by the reference value of the equation dependent variable. Therefore, normalized residuals are equivalent to dimensionless variables changes in a simple Jacobi iteration. These options guarantee that the numerical error is dominated by the discretization error.

[2]In this paper we only address time-averaged RANS, i.e. statistically steady flow.

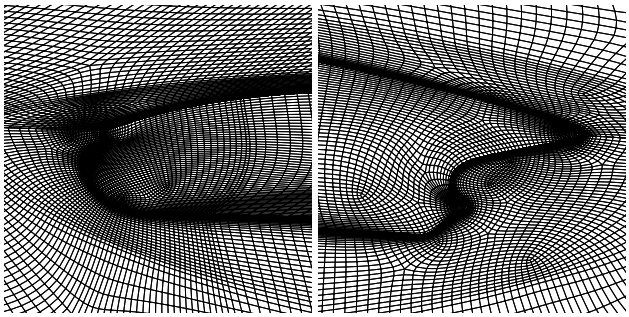

FIGURE 3. Illustration of coarsest grid at the bow and stern regions of the KVLCC2 tanker.

RESULTS

All the results presented in the following sections are dimensionless quantities with ρ, L_{PP} and V_∞ as the reference quantities. It must be stated that results from simulations performed with different values of V_x at the inlet ($\pm 0.25\%$ and $\pm 0.5\%$) also use the nominal value of V_∞ as the reference velocity.

Grid sets

A set of 10 nearly-geometrical multi-block structured grids was generated with the GridPro package [17]. The grids range from 0.764545×10^6 to 47.612928×10^6 cells and the maximum near-wall cell height in wall coordinates $y^+_{\max}$ varies between 0.6 (coarsest grid) and 0.15 (finest grid). Fig. 3 illustrates the coarsest grid at the bow and stern regions.

The grid refinement ratio r_i is determined from the total number of cells N_{cells}

$$r_i = \frac{h_i}{h_1} = \left(\frac{N_{cells_1}}{N_{cells_i}} \right)^{\frac{1}{3}} , \tag{6}$$

where h stands for the typical cell size (with 1 denoting the finest grid). In the present grid set, $1 \leq r_i \leq 4.0$.

Reference solution

The estimation of the discretization error of the selected quantities of interest requires an exact solution that is not available. In this study power series expansions [6] are used to obtain a reference ("exact") solution ϕ_o using

$$\phi_i = \phi_o + \alpha r_i^p . \tag{7}$$

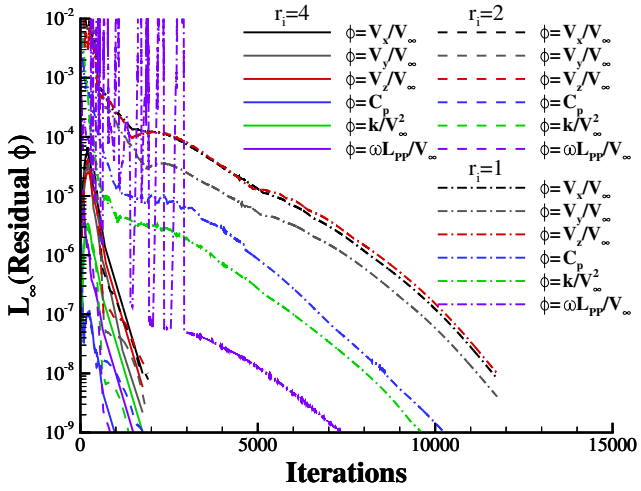

FIGURE 4. Iterative convergence of the numerical solutions performed in the grids with $r_i = 4$, $r_i = 2$ and $r_i = 1$ for the simulation of the flow around the KVLCC2 tanker at model scale Reynolds number.

ϕ_i represents a quantity of interest determined in the grid with refinement r_i, α is a constant and p is the observed order of grid convergence. Eq. (7) is solved in the least-squares sense [6] using the numerical results of the six finest grids that cover a grid refinement ratio of two, $1 \leq r_i \leq 2$. As described in [6], p is limited to values between 0.5 and 2.0. Furthermore, in cases where the least squares solution is unable to determine p (non monotonic convergence) ϕ_o is estimated from

$$\phi_i = \phi_o + \alpha_1 r_i + \alpha_2 r_i^2 \,, \tag{8}$$

where α_1 and α_2 are constants.

Iterative convergence

Although iterative errors are reduced to negligible levels in the present study, it is important to illustrate the convergence history of the simulations. Fig. 4 presents the L_∞ norm of the normalized residuals of all the transport equations for the grid refinement levels $r_i = 4$, $r_i = 2$ and $r_i = 1$. All calculations satisfied the selected iterative convergence criteria. Nonetheless, the iterative convergence rate decreases with the reduction of r_i, especially for the finest grid ($r_i = 1$). Furthermore, the convergence of ω in the finest grid includes several overshoots before exhibiting a smooth convergence.

Discretization errors

The convergence of the friction C_F and pressure C_P resistance coefficients with grid refinement is illustrated in Fig. 5. Both coefficients exhibit monotonic convergence with the observed order of grid convergence slightly larger than one for C_F

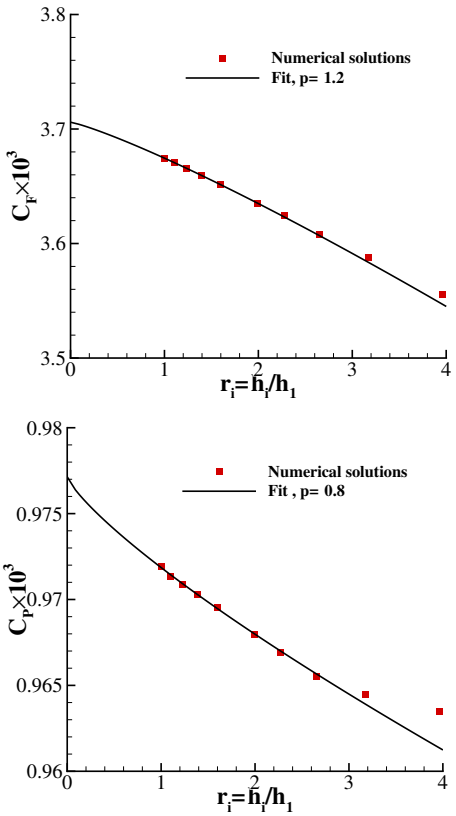

FIGURE 5. Convergence of the friction C_F and pressure C_P resistance coefficients with grid refinement r_i in the simulation of the flow around the KVLCC2 tanker at model scale Reynolds number.

TABLE 1. Estimated discretization errors e_{disc} of the friction C_F and pressure C_P resistance coefficients at three different grid refinement r_i levels. Flow around the KVLCC2 tanker at model scale Reynolds number.

$e_{disc}(\%)$	$r_i = 1$	$r_i = 2$	$r_i = 4$
C_F	-0.85	-1.93	-4.09
C_P	-0.53	-0.94	-1.41

and slightly lower than one for C_P. Table 1 presents the estimates of the discretization errors e_{disc} of C_F and C_P for $r_i = 1$, $r_i = 2$ and $r_i = 4$ as a percentage of the values obtained in the finest grid. For these integral quantities, the estimated discretization errors are below 1% for the finest grid ($r_i = 1$), but there is a clear increase of e_{disc} with grid coarsening, especially for C_F.

Naturally, we cannot present the convergence with grid refinement of the four local flow quantities (V_x, V_y, V_z and k) at the 654 locations of the propeller plane ($x = 0.0175 L_{PP}$). Therefore,

TABLE 2. Mean $\overline{e}_{disc}$ and standard deviation $\sigma_{e_{disc}}$ of the absolute value of the estimated discretization errors $|e_{disc}|$ for the Cartesian velocity components (V_x/V_∞, V_y/V_∞ and V_z/V_∞) and turbulence kinetic energy k/V_∞^2 at the 654 locations of the propeller plane ($x = 0.0175L_{PP}$). Flow around the KVLCC2 tanker at model scale Reynolds number.

	V_x/V_∞		V_y/V_∞	
r_i	$\overline{e}_{disc} \times 10^2$	$\sigma_{e_{disc}} \times 10^2$	$\overline{e}_{disc} \times 10^2$	$\sigma_{e_{disc}} \times 10^2$
1	0.61	1.59	0.19	0.49
2	1.02	1.94	0.30	0.60
4	1.49	2.57	0.47	0.97

	V_z/V_∞		k/V_∞^2	
r_i	$\overline{e}_{disc} \times 10^2$	$\sigma_{e_{disc}} \times 10^2$	$\overline{e}_{disc} \times 10^3$	$\sigma_{e_{disc}} \times 10^3$
1	0.23	0.50	0.31	1.01
2	0.39	0.65	0.58	1.33
4	0.60	1.18	1.00	1.86

we characterize the discretization errors of these variables with the histograms of the signed estimated value of e_{disc} in Fig. (6) and the mean and standard deviations of the absolute value of $|e_{disc}|$ presented in Table 2.

The results exhibit a similar behaviour for the four variables with almost an equivalent number of locations exhibiting positive or negative errors. There is a systematic increase of $\overline{e}_{disc}$ and $\sigma_{e_{disc}}$ with the increase of r_i, but the mean values of the estimated discretization errors do not double when the refinement ratio is multiplied by 2, which would be roughly the expected behaviour for first order convergence. However, estimating the observed order of grid convergence p for the present level of grid refinement (six grids between 6×10^6 and 47.6×10^6 cells) is not trivial. Four different alternatives are used to obtain the data included in Fig. 6 and Table 2 [6]: p obtained from the data; $p = 1$; $p = 2$ and 2 terms as defined in Eqn. (8). Table 3 presents the percentage of locations determined with each of these alternatives.

The data presented in Table 3 confirms the difficulties to estimate p for local quantities of complex turbulent flows calculated with the RANS equations. Surprisingly, k is the variable that exhibits more locations where p is determined from the data, but it is still less than 30% of the locations. Nonetheless, the average value of p estimated from the data is close to 1.3 for the four flow variables. On the other hand, the results also indicate that are still roughly 10% of the locations where the solutions are not converging monotonically for grids with more than 6×10^6 cells, which presents again a challenge for the estimation of discretization errors.

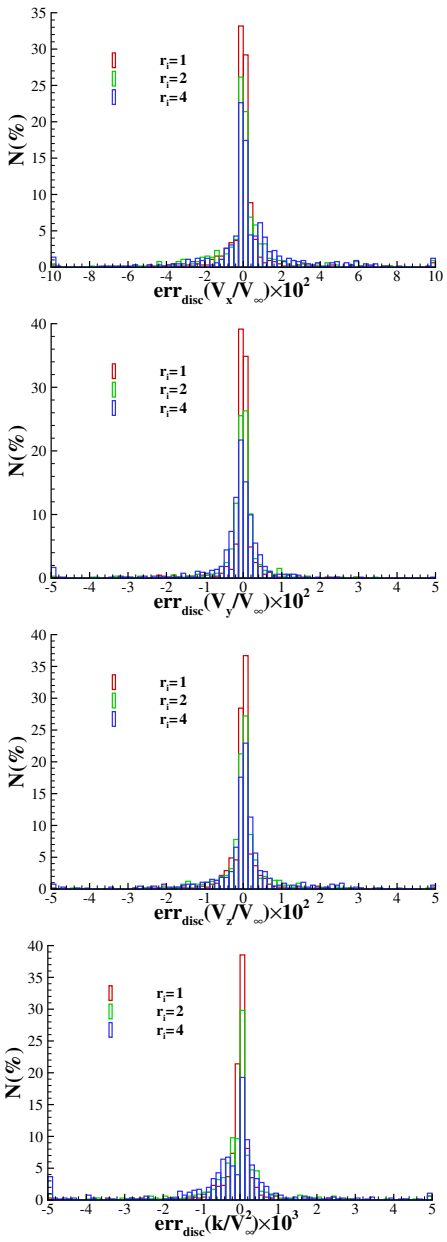

FIGURE 6. Histograms of the signed estimated value of e_{disc} for the Cartesian velocity components (V_x, V_y and V_z) and turbulence kinetic energy k at the 654 locations of the propeller plane ($x = 0.0175L_{PP}$). Flow around the KVLCC2 tanker at model scale Reynolds number.

Sensitivity coefficients

As for the study reported in [1], the main goal of this study is to address the influence of numerical (discretization) errors on the estimation of the sensitivity coefficients of the quantities of

TABLE 3. Percentage of cases for the four alternatives used in the estimation of the discretization errors e_{disc}. Cartesian velocity components (V_x/V_∞, V_y/V_∞ and V_z/V_∞) and turbulence kinetic energy k/V_∞^2 at the 654 locations of the propeller plane ($x = 0.0175L_{PP}$). Flow around the KVLCC2 tanker at model scale Reynolds number.

	Eqn. (7)			Eqn. (8)
Variable	p data	$p=1$	$p=2$	2 terms
V_x	15.7	30.4	44.8	9.1
V_y	18.5	25.7	45.0	10.8
V_z	16.4	27.7	46.0	9.9
k	29.7	14.5	43.3	12.5

TABLE 4. Sensitivity coefficients of the friction C_F and pressure C_P resistance coefficients obtained for three levels of grid refinement r_i. Δ stands for $\left((V_\infty)_p - (V_\infty)_m\right)/V_\infty$, C_{F_o} and C_{P_o} stand for the values obtained in the finest grid $r_i = 1$ using the nominal value of V_∞. Flow around the KVLCC2 tanker at model scale Reynolds number.

	$S(C_F)_{V_\infty} \times V_\infty/C_{F_o}$		$S(C_P)_{V_\infty} \times V_\infty/C_{P_o}$	
r_i	$\Delta = 0.005$	$\Delta = 0.01$	$\Delta = 0.005$	$\Delta = 0.01$
1	1.839	1.839	1.786	1.786
2	1.813	1.813	1.771	1.771
4	1.763	1.763	1.754	1.755

interest using central-differences that lead to

$$S(\phi)_{V_\infty} = \frac{\partial \phi}{\partial V_\infty} \simeq \frac{\phi_p - \phi_m}{(V_\infty)_p - (V_\infty)_m} , \tag{9}$$

where ϕ stands for the quantity of interest and the subscripts $_p$ and $_m$ identify the two extra simulations performed to obtain the sensitivity coefficient. In this case we have used $((V_\infty)_p - (V_\infty)_m) = 0.01V_\infty$ and $((V_\infty)_p - (V_\infty)_m) = 0.005V_\infty$ to apply Eqn. (9) for all selected quantities of interest using three grid refinement levels: $r_i = 1$, $r_i = 2$ and $r_i = 4$. All sensitivity coefficients are presented in dimensionless form, which means that $S(\phi)_{V_\infty}$ is multiplied by V_∞ and divided by ϕ_o that corresponds to the quantity of interest obtained in the finest grid ($r_i = 1$) using the nominal value of V_∞.

Table 4 presents the sensitivity coefficients obtained for the resistance coefficients C_F and C_P using the two different intervals of $((V_\infty)_p - (V_\infty)_m)$. The sensitivity coefficients obtained from the two intervals are (almost) identical and indicate that a change of 1% in the value of V_∞ produces a change of the resistance coefficients of approximately 1.8%. On the other hand, the influence of the grid refinement level on $S(C_F)$ is larger than on $S(C_P)$ with the main differences obtained between the $r_i = 1$ and $r_i = 4$ solutions, as expected. However, the largest differences between dimensionless sensitivity coefficients are smaller than 0.07, which is not a completely unexpected result considering that the convergence of the two variables illustrated in Fig. 5 is smooth and monotonic.

TABLE 5. Number of cases with an absolute percentual change of $S(\phi)_{V_\infty}$ obtained with $r_i = 2$ or $r_i = 4$ when compared to $S(\phi)_{V_\infty}$ determined with $r_i = 1$ larger than 5%. Results for the Cartesian velocity components (V_x, V_y and V_z) and turbulence kinetic energy k at the 363 locations of the propeller plane ($x = 0.0175L_{PP}$ that exhibit $V_x \leq 0.9V_\infty$). Flow around the KVLCC2 tanker at model scale Reynolds number.

r_i	V_x	V_y	V_z	k
2	9.85	25.1	29.8	54.7
4	24.1	36.7	49.7	88.7

Addressing the effect of discretization errors on the estimation of the sensitivity coefficients of the local quantities of interest is more troublesome. There are four variables (V_x, V_y, V_z and k) at 654 locations and so the data must be handled statistically. The percentual change of $S(\phi)_{V_\infty}$ obtained with $r_i = 2$ or $r_i = 4$ when compared to $S(\phi)_{V_\infty}$ determined with $r_i = 1$ is calculated from

$$R_S(\phi) = \left(\frac{S(\phi)_{V_\infty}(r_i)}{S(\phi)_{V_\infty}(r_1)} - 1 \right) \times 100 . \tag{10}$$

$R_S(\phi)$ is determined only at the 363 locations that exhibit $V_x \leq 0.9V_\infty$ to avoid the region where viscous effects are negligible. The results are presented in Fig. 7 that includes the cumulative density functions (CDFs) of $R_S(V_x)$, $R_S(V_y)$, $R_S(V_z)$ and $R_S(k)$.

The results obtained with the two intervals of V_∞ tested are graphically identical. The variable that shows the smallest influence of the discretization error on the estimation of the sensitivity coefficients is V_x, whereas $S(k)_{V_\infty}$ exhibits the largest changes with r_i. The CDFs of $R_S(\phi)$ are not symmetric (that would mean CDF=50% for $R_S(\phi) = 0$) and the shape of the CDF depends on the selected flow variable and level of grid refinement. Nonetheless, it is clear that for the present levels of grid refinement tested the sensitivity coefficients are dependent on the numerical (discretization) error.

Table 5 presents the percentage of cases that exhibits $|R_S(\phi)|$ larger than 5%. It is clear that the effect of the numerical (discretization) error on the determination of $S(\phi)_{V_\infty}$ is not negligi-

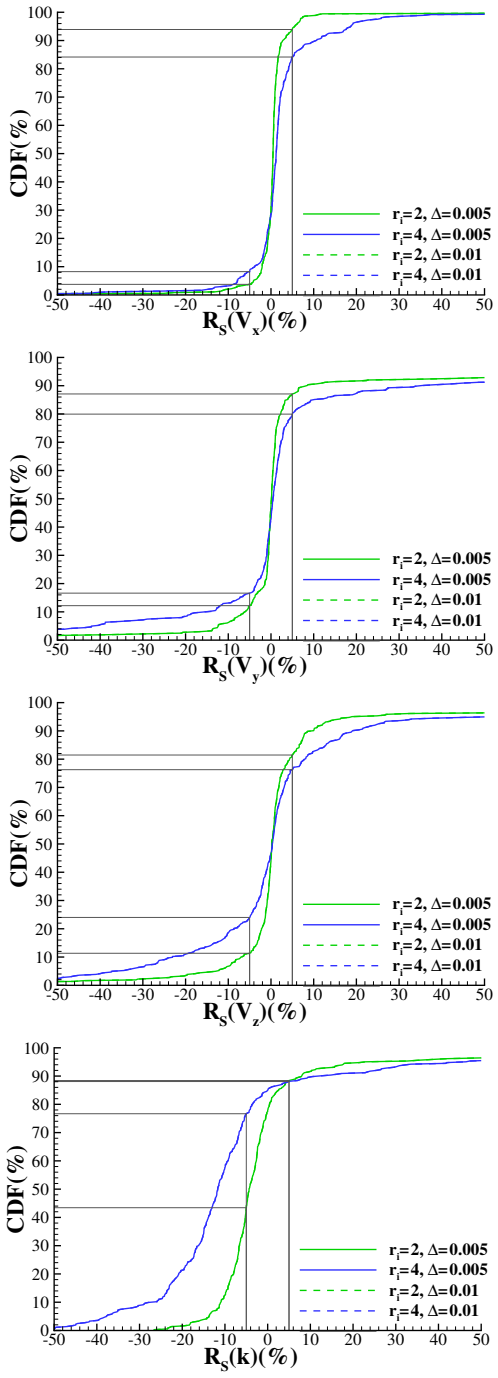

FIGURE 7. Cumulative density functions of the percentual change of $S(\phi)_{V_\infty}$ obtained with $r_i = 2$ or $r_i = 4$ when compared to $S(\phi)_{V_\infty}$ determined with $r_i = 1$. Results for the Cartesian velocity components (V_x, V_y and V_z) and turbulence kinetic energy k at the 363 locations of the propeller plane ($x = 0.0175L_{PP}$ that exhibit $V_x \leq 0.9V_\infty$). Flow around the KVLCC2 tanker at model scale Reynolds number.

ble. The estimation of the k sensitivity coefficients on the coarsest grid ($r_i = 4$) may be completely misleading and the same observation also applies to the V_y and V_z velocity components.

CONCLUSIONS

This paper presents a study about the dependence of the estimation of sensitivity coefficients on the numerical (discretization) error, which assesses the independence of numerical and input uncertainties. The test case is the flow around the KVLCC2 tanker at model scale Reynolds number and the quantities of interest include integral parameters (resistance coefficients) and local variables (Cartesian velocity components and turbulence kinetic energy) at the propeller plane.

Grid refinement studies were performed with grids ranging from 0.76×10^6 and 47.6×10^6 cells using the time-averaged RANS equations supplemented by the $k-\omega$ SST two-equation eddy-viscosity turbulence model. Sensitivity coefficients are evaluated for three levels of grid refinement: $r_i = 1$ (finest grid); $r_i = 2$ and $r_i = 4$ (coarsest grid).

The results suggest the following conclusions:

The grid refinement level to obtain negligible discretization errors in RANS solutions of complex turbulent flows is most likely much more demanding than the typical values published in the open literature.

For "practical applications" including turbulent flows, the determination of sensitivity coefficients in coarse grids may lead to results significantly polluted by discretization errors.

ACKNOWLEDGEMENT

The fourth author acknowledges the financial support provided by Fundação para a Ciência e Tecnologia through a research grant under the Bolsas de Doutoramento and Pós-Doutoramento 2016 program. We also acknowledge the funding of the Dutch Ministry of Economic Affairs. This work has been approved by LANL for unlimited release, with release code LA-UR-20-20700.

REFERENCES

[1] L. Eça, R. Lopes, F.S. Pereira, G. Vaz - *Numerical and parameter uncertainties: are they independent?* - in Proceedings of ASME 2019 Verification and Validation Symposium, May 17-22, 2019, Las Vegas, Nevada, USA.

[2] ASME V&V 20-2009 (R2016), Standard for Verification and Validation in Computational Fluid Dynamics and Heat Transfer, The American Society of Mechanical Engineers (ASME), New York.

[3] `www.refresco.org`

[4] Menter F.R., Kuntz M., Langtry R. - *Ten Years of Industrial Experience with the SST Turbulence Model* - Turbulence, Heat and Mass Transfer 4, ed: K. Hanjalic, Y. Nagano, and M. Tummers, Begell House, Inc., 2003, pp. 625 - 632.

[5] Lee, S., Kim, H., Kim, W., Van, S. *Wind tunnel tests on flow characteristics of the KRISO 3,600 TEU containership and 300K VLCC2 double-deck ship models*- Journal of Ship Research. Vol. 47 (1) 2003, 2438.

[6] Eça L., Hoekstra M. - *A Procedure for the Estimation of the Numerical Uncertainty of CFD Calculations Based on Grid Refinement Studies*, Journal of Computational Physics, Volume 262, 2014, pp. 104-130.

[7] Larsson L., Stern F., Bertram V. (Eds.) *Gothenburg 2000 - A Workshop on Numerical Hydrodynamics*. Chalmers University of Technology, Gothenburg, 2000, Sweden.

[8] Larsson L., Stern F., Visonneau M. (Eds.), *Gothenburg 2010 - A Workshop on Numerical Ship Hydrodynamics*. Chalmers University of Technology, Gothenburg, 2010, Sweden.

[9] Pereira F.S., Eça L. and Vaz G., *Verification and Validation exercises for the flow around the KVLCC2 tanker at model and full-scale Reynolds numbers*, Ocean Engineering, Volume 129, January 2017, pp 133-148.

[10] Pereira F.S., Eça L., Vaz G. and Kerkvliet M, *Application of second-moment closure to statistically steady flows of practical interest*, Ocean Engineering, Volume 189, October 2019.

[11] Eça L, Hoekstra M. *On the Grid Sensitivity of the Wall Boundary Condition of the $k-\omega$ model*. Journal of Fluids Engineering, Vol. 126, N^o 6, November 2004, pp. 900-910.

[12] Wilcox D.C. *Turbulence Modelling for CFD*, 2nd ed., DCW Industries, 2006.

[13] Vaz G., Jaouen F. and Hoekstra M. *Free-Surface Viscous Flow Computations. Validation of URANS Code FRESCO*. In Proceedings of OMAE2009, Honolulu, Hawaii, USA, June 2009.

[14] Klaij C.M., Vuik C. *SIMPLE-type preconditioners for cell-centered, collocated finite volume discretization of incompressible Reynolds-averaged Navier-Stokes equations*. International Journal for Numerical Methods in Fluids 71(7):830849, 2013.

[15] Miller T.F., Schmidt F.W. *Use of a pressure weighted interpolation method for the solution of the incompressible Navier-Stokes equations on a nonstaggered grid system*. Journal of Numerical Heat Transfer, Vol 14, 1988, pp. 213-233.

[16] Eça L., Klaij C.M., Vaz G., Hoekstra M., Pereira F.S. *On Code Verification of RANS Solvers*. Journal of Computational Physics, Volume 310, Issue C, April 2016, pp. 418-439.

[17] `www.gridpro.com`